A Simplified Model to Predict Oxygen Attenuation on Earth-space Links

Lorenzo Luini, *Senior Member, IEEE,* and Carlo Riva, *Senior Member, IEEE*

Abstract— **A simplified yet accurate model to predict oxygen attenuation for Earth-space applications (10-350 GHz range) is presented in this contribution. The model is developed by taking advantage of an extensive set of high-resolution radiosonde observations (RAOBS) collected in several sites worldwide. It predicts the statistics of oxygen attenuation along the path by retaining the accurate formulation for the specific oxygen attenuation included in the Liebe MPM93 model, but it relies on simplified meteorological input values (namely the mean yearly ground temperature and the statistics of the ground water vapor content), rather than on full atmospheric vertical profile. Tested against attenuation estimates obtained from Liebe MPM93 model coupled with the mentioned RAOBS data, the model provides a very good prediction accuracy in the full 10-350 GHz range, which turns out to be almost independent of the considered site.**

Index Terms— **Electromagnetic wave propagation, oxygen attenuation, atmospheric effects, Earth-space links**

I. INTRODUCTION

THE complexity of satellite communication (SatCom) systems is progressively increasing in order to accommodate the users' request, which is slowly shifting from simple TV broadcast to more comprehensive interactive services (e.g. Internet via satellite, contents on demand, …) [1]. The key requirement to deliver such services is large bandwidth, which is available at higher frequency bands (e.g. Ka, for gateways and users links, and Q and V for gateways in the near future), at the expense of a strong increase in the atmospheric impairments [2]. Among them, the attenuation induced by rain has an extremely detrimental impact, especially in the millimeter-wave range; nevertheless, it is of paramount importance to devise accurate models for the prediction of the effect of any constituent interacting with electromagnetic waves, i.e. also clouds, water vapor and oxygen [3]. In fact, as frequency increases, it is progressively more critical to guarantee high levels of system availability, such that even small differences in the power margin aimed at coping with atmospheric impairments might have a determinant role on the link quality. In addition, although

gases definitely have a reduced contribution to total attenuation if compared to clouds and hydrometeors, (save for frequencies around absorption peaks, e.g. roughly 60 GHz for oxygen and 22 GHz for water vapor), they are always present in the atmosphere. When low-elevation angle applications are concerned (e.g. links between ground stations and Medium/Low Earth Orbit satellites [4]), even in absence of clouds, the gaseous attenuation might amount to several dBs (especially in tropical/equatorial sites) [5]. As a matter of fact, any upgrade in the models' prediction accuracy can yield a significant improvement in estimating the link performance.

The most accurate and acknowledged methods to predict the attenuation induced by oxygen, A_{OX}, are mass absorption models: typical examples are the methods proposed by *Liebe et al.* (MPM93 [6]) and Roserkranz [7], for the 1-1000 GHz frequency range, or methodologies implemented in popular simulation software packages (e.g. MODTRAN®4 [8] and LBLRTM [9]), which, however, are intended to be used mostly for the THz range [10]. These methodologies integrate along the path the specific attenuation due to oxygen γ_{OX}, whose variation along the profile is taken into due account by employing vertical profiles of pressure (P), temperature (T) and relative humidity (RH), typically collected using radiosondes.

The Liebe's MPM93 model is currently adopted by the ITU-R (International Telecommunication Union – Radiocommunication sector) in Annex 1 of Recommendation P.676-11 [11]. Due to the difficulty in retrieving *P-RH-T* vertical profiles worldwide and the complexity of such a method, the same Recommendation includes (in Annex 2) also an approximate A_{OX} prediction approach, which relies on mean yearly values of the ground temperature, pressure and relative humidity and on the definition of the oxygen equivalent height, taking into account, in a simplified way, the variation of γ_{OX} with height. Actually, this prediction method has a limited applicability (altitudes below 10 km) and accuracy (particularly degraded in some bands, such as 50-70 GHz) and it estimates only the mean yearly value of A_{OX}.

This work aims at overcoming such limitations by presenting an alternative simplified prediction model for Earth-space links operating in the 10-350 GHz frequency range. Specifically, the proposed method, developed by taking advantage of an extensive set of high-resolution radiosonde observations (RAOBS) collected in 24 sites worldwide, maximizes the prediction accuracy in the whole 10-350 GHz

frequency range and provides as output the full Complementary Cumulative Distribution Function (CCDF) of A_{OX}. However, the method still relies on simplified meteorological input values: the mean yearly ground temperature and the CCDF of the ground water vapor content (both of which are already available in terms of global digital maps attached to ITU-R recommendations [12],[13]).

The remainder of the paper is organized as follows: Section II presents the RAOBS dataset, while the central part of the work lies in Section III, briefly recalling the MPM93 model and presenting the new prediction model; its accuracy is tested in Section IV, while Section V draws some conclusions.

II. THE RADIOSONDE OBSERVATION DATASET

RAOBS are a source of paramount importance for atmospheric sciences (for instance, they are assimilated into Numerical Weather Prediction – NWP – models), but are also of a very useful means to study the Earth-space propagation of electromagnetic waves, as they allow to quantify the effects induced by atmospheric gases such as water vapor and oxygen using accurate mass absorption models [6],[7]. In this contribution, we take advantage of a large set of RAOBS data collected in 24 sites across the Globe, for ten years and characterized by high accuracy and fine vertical resolution.

The RAOBS dataset used in this work was extracted from the NCAR (National Center for Atmospheric Research) database. More in detail, it includes vertical profiles of pressure, temperature and relative humidity, collected regularly twice a day between 1980 and 1989 in 24 sites across the Globe. Table I lists the details of the sites where radiosondes were launched, showing coverage of different latitudes, e.g. high (Finland) to equatorial (Singapore) ones.

Additional details on the RAOBS database are included in [14], where the data validation is duly described. As an example of the preprocessing procedures applied, RAOBS levels showing inversions of pressure were excluded and outliers of integrated parameters (e.g. the total water vapor content) were discarded.

TABLE I.   GEOGRAPHICAL COORDINATES AND ALTITUDE OF THE SITES WHERE RAOBS DATA WERE COLLECTED.

Station number	Station name	Country code	Latitude (° N)	Longitude (° E)	Altitude (m a.m.s.l.)
1	Sodankyla	FI	67.22	26.39	178
2	Jokionen	FI	60.49	23.30	103
3	Stornoway	UK	58.13	353.41	14
4	Hemsby	UK	52.41	1.41	13
5	De Bilt	NL	52.06	5.11	2
6	Uccle	BX	50.48	4.21	104
7	Lyon	FR	45.44	5.05	240
8	Berlin	DE	52.29	13.25	46
9	Wien	OS	48.15	16.22	200
10	Milan	IT	45.26	9.17	107
11	Brindisi	IT	40.39	17.57	7
12	Trapani	IT	37.55	12.30	5
13	Cagliari	IT	39.15	9.03	4
14	Moscow	RUS	55.45	37.34	184
15	Tabuk	SD	28.22	36.35	771
16	Delhi	IN	28.35	77.12	281
17	Hong Kong	CH	22.19	114.10	65
18	Singapore	SR	1.22	103.59	14
19	Dal-El-Beida	AL	36.43	3.15	25
20	Cape Town	ZA	-33.58	18.36	46
21	San Diego	US (CA)	32.49	242.52	124
22	Denver	US (CO)	39.45	255.08	1611
23	Mexico City	MX	19.26	260.55	2231
24	Lihue-On-Kauai	US (HI)	21.59	200.39	36

III. ATTENUATION INDUCED BY OXYGEN

A. The reference methodology

Mass absorption models, among which those proposed by Liebe *et al.* (MPM93) [6] and by Rosenkranz [7] are worth being cited, provide accurate estimate of the attenuation due to oxygen by considering the microphysical interaction between the gas molecules and electromagnetic waves: at specific frequencies (typically referred to as "lines"), resonant effects are triggered, which causes high absorption of electromagnetic energy. More in detail, the specific attenuation γ_{OX} depends on pressure P, temperature T and water vapor content v. As a result, in order to accurately estimate γ_{OX}, knowledge of the full P, T and v (or relative humidity RH, from which v can be derived) vertical profiles is required (e.g. as obtained from radiosondes). Given their accuracy, gaseous attenuation results derived from mass absorption models are typically considered as the reference against which prediction models are evaluated.

The current ITU-R recommendation devoted to the prediction of the attenuation due to atmospheric gases (P.676-11 [11]) includes, in Annex 1, the MPM93 model expressions to calculate the path attenuation due to oxygen A_{OX}. Without reporting all the equations (which can be found both in [6] and [11]), the specific attenuation γ_{OX} consists of the contribution

of 44 absorption lines (from roughly 50 to 840 GHz), whose intensity and shape vary from peak to peak and as a function of P, T and v. Moreover, γ_{OX} also includes a dry air continuum term, which, for frequencies f above 10 GHz, is due to pressure-induce nitrogen attenuation. Fig. 1 reports the trend of γ_{OX} (dB/km) with frequency, for two sample sets of input values: the impact of oxygen is generally quite limited, but the attenuation reaches extreme values close to the absorption peaks at 61.15 GHz (more than 10 dB/km) and 118.75 GHz (roughly 1 dB/km), and it is definitely not negligible for frequencies around such peaks (approximately 0.1 dB/km at 50 and 70 GHz).
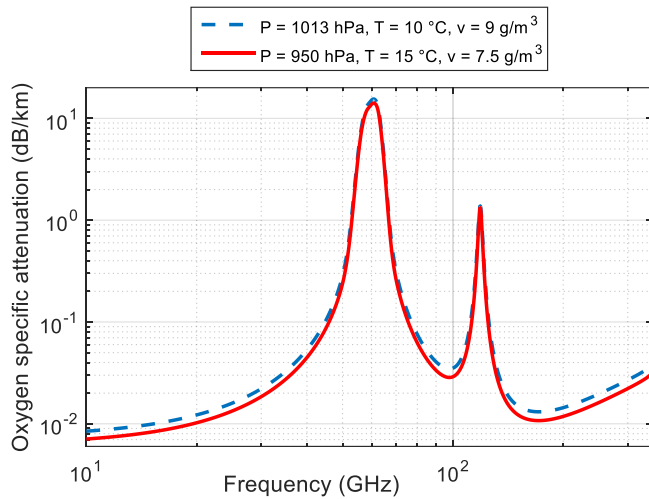

Fig. 1. Trend of the specific attenuation due to oxygen with frequency (10-350 GHz) for two atmospheric conditions: $P = 1013$ hPa, $T = 10°C$, $v = 9$ g/m^3 (blue dashed line); $P = 950$ hPa, $T = 15°C$, $v = 7.5$ g/m^3 (red solid line).

B. The ITU-R approximate method

Given the complexity of the method in Annex 1 of ITU-R P.676-11, the same Recommendation proposes an approximate approach to calculate A_{ox}, which is simply given by:

$$A_{OX} = \gamma_{OX}(f, \overline{T}_G, \overline{v}_G, \overline{P}_G) h_0(f, \overline{P}_G) \qquad (1)$$

where γ_{OX} (dB/km) is a function of the frequency f, and of the mean yearly values of temperature, water vapor content, and pressure, at the ground level ($\overline{T}_G$, $\overline{v}_G$ and $\overline{P}_G$, respectively). The calculation of γ_{OX} is the same as in Annex 1, though slightly simplified (omission of the Zeeman splitting of oxygen lines [11]). On the other side, h_0 (km), only function of f and $\overline{P}_G$, is the equivalent height, defined so as to consider the variation of γ_{OX} with height h.

The simplified model proposed in Annex 2 presents three main limitations: it is applicable to altitudes below 10 km (which is linked to the simplified calculation of γ_{OX}), it provides only the mean yearly value of A_{OX} (not the full Complementary Cumulative Distribution Function – CCDF, as

e.g. for the ITU-R methods predicting cloud [15] and water vapor attenuation [11]), and, finally, its accuracy (if compared to the predictions obtained from the Annex 1 method), though generally within ±10%, can be much degraded in the 50-70 GHz band, as clearly stated in the Recommendation. Among these limitations, the last one is of crucial importance: though no Earth-space systems are expected to operate around 60 GHz due to the extremely high absorption values (path attenuation higher than 100 dB for zenithal links), a proper prediction of A_{OX} at frequencies around 50 and 70 GHz (far from being negligible as shown in Section II.A) is of key importance for the design of possible future systems working in the V band. Indeed, the 47.5-51.4-GHz and 71-76-GHz bands have been already allocated by ITU-R to fixed and mobile satellite services [16].

C. The new prediction model

1) Rationale of the model

The new prediction model aims at overcoming the limitations of the current Annex 2 method pointed out in the previous section, yet aiming at a simplified approach. Specifically it provides global prediction of the full CCDF of A_{OX} as a function of $\overline{T}_G$, $\overline{P}_G$, and of the CCDF of the water vapor content at the ground, v_G. This is achieved by using γ_{OX} of Annex 1, and by introducing a new expression for h_0. Details on the development of the new model are provided in the next sections.

2) Vertical profile of the specific attenuation due to oxygen

The extensive RAOBS dataset described in Section II was first used to investigate the trend of the specific oxygen attenuation with height. Fig. 2 shows a sample vertical profile of γ_{OX}, for Milano Linate, obtained by using the vertical profiles of P, T and RH as input to the MPM93 model.
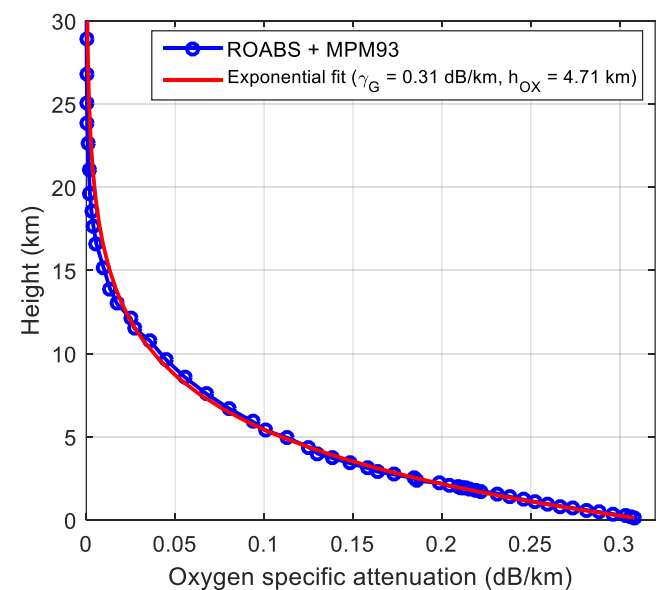

Fig. 2. Sample profile of specific attenuation at 50 GHz calculated using the MPM93 model [6] and the P-RH-T vertical profiles measured by the

radiosonde launched at Milano Linate airport (blue circles) and its exponential fit (red curve).

It is clear from the figure that the γ_{OX} profile can be accurately modeled by an exponential expression:

$$\gamma_{OX}(h) = \gamma_G \exp(-h/h_{OX}) \tag{2}$$

where γ_G (dB/km) is the oxygen specific attenuation relative to the ground, while h_{OX} (km), typically named scale height, regulates the decay of γ_{OX} with height. The legend in Fig. 2 reports γ_G and h_{OX} obtained by fitting the expression in (2) to the RAOBS-derived γ_{OX} profile. For the sake of comparison, the equivalent height, calculated according to Annex 2 of ITU-R P.676-11 (see (1)) is $h_0 = 5.07$ km.

Starting from (2), the zenithal path attenuation due to oxygen is obtained by integrating γ_{OX} vertically:

$$A_{OX} = \int_{0 \text{ km}}^{\infty} \gamma_G \, e^{-h/h_{OX}} \, dh = \gamma_G \, h_{OX} \tag{3}$$

According to (3), the oxygen scale height is equal to the equivalent height, and can be used, together with the ground specific attenuation due to oxygen, to accurately approximate A_{OX}. As an example, for the profile shown in Fig. 2, $A_{OX} = 1.37$ dB and 1.46 dB (roughly 5% of percentage difference) according to the MPM93 model and equation (3), respectively, where, as indicated in the legend of Fig. 2, $\gamma_G = 0.31$ dB/km and $h_{OX} = 4.71$ km.

3) Oxygen scale height

This section investigates the dependence of the oxygen scale height on frequency, as well as on ground pressure, temperature and water vapor content, in order to define an analytical expression to relate h_{OX} to simple local meteorological inputs. To this aim, the full set of RAOBS data was exploited (see Table I). Specifically, h_{OX} was calculated for each ascent of each RAOBS station by fitting equation (2) to the MPM93-derived vertical profile of γ_{OX} (see Fig. 2). This exercise was repeated for frequencies ranging from 10 GHz (limit below which the zenithal path attenuation due to oxygen falls below 0.05 dB) to 350 GHz (the limit of validity for the approximated method in Annex 2 of ITU-R P.676-11). The trend of h_{OX} with frequency is reported in Fig. 3, which specifically shows the average value of h_{OX} (μ) and standard deviation (σ) bounds.
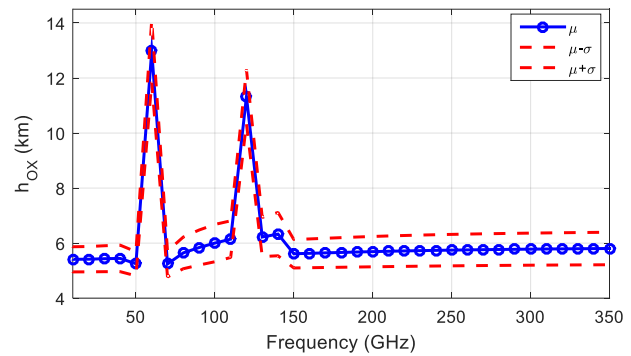

Fig. 3. Trend of the average value of h_{OX} as a function of frequency, together with standard deviation (σ) bounds.

It is clear from the results that h_{OX} shows a sudden increase near the oxygen absorption peaks (centered around 61.15 GHz and 118.75 GHz), while it is rather constant for $f < 50$ GHz and $f > 150$ GHz, with μ ranging between 5.5 and 6 km. Indeed, around absorption peaks, γ_{OX} along the whole profile increases considerably, and its decrease with ~~frequency~~ height becomes less steep than the one on Fig. 2, i.e. h_{OX} increases.

Further analyses have indicated a positive correlation of h_{OX} both with T_G (ground temperature) and v_G. Specifically, Fig. 4 shows that h_{OX} is approximately a linear function of T_G, while Fig. 5 indicates that the relationship between h_{OX} and v_G follows a power-law (gray scale density scatter plot, higher concentration in darker areas). In both figures, results are relative to all stations, but to a single frequency (50 GHz): the same trends were found in the whole 10-350 GHz range.
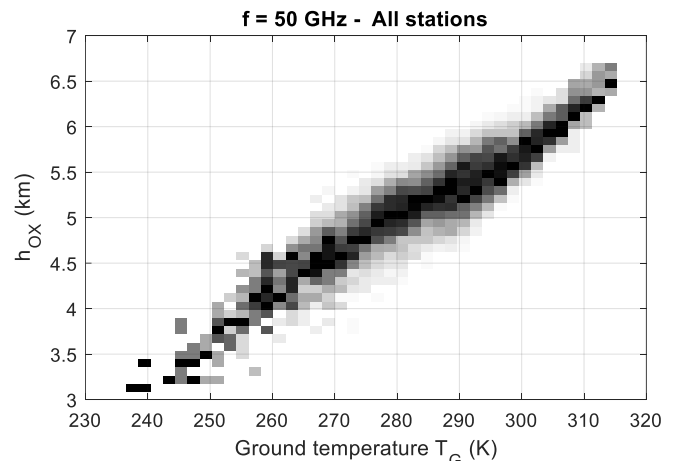

Fig. 4. Correlation between the ground pressure T_G and h_{OX} at $f = 50$ GHz (all stations considered); gray scale density scatter plot, higher concentration in darker areas.
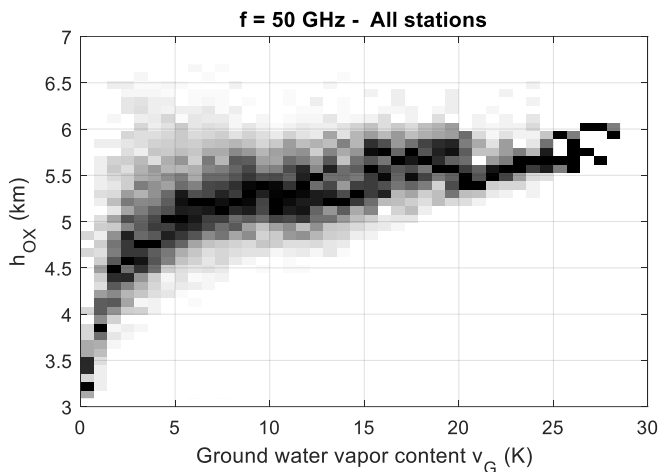
Fig. 5. Correlation between the ground pressure v_G and h_{OX} at $f = 50$ GHz (all stations considered); gray scale density scatter plot, higher concentration in darker areas.

On the contrary, almost no correlation was found between h_{OX} and P_G, as shown in Fig. 6. The different "zones" clearly discernible in Fig. 6 are associated to stations lying at different altitudes (see Table I). In fact, while the height of most sites is lower than 300 m a.m.s.l., Tabuk (SD), Denver (USA) and Mexico City (MX) are more elevated (771 m, 1611 and 2231 m), i.e. associated to lower values of P_G.
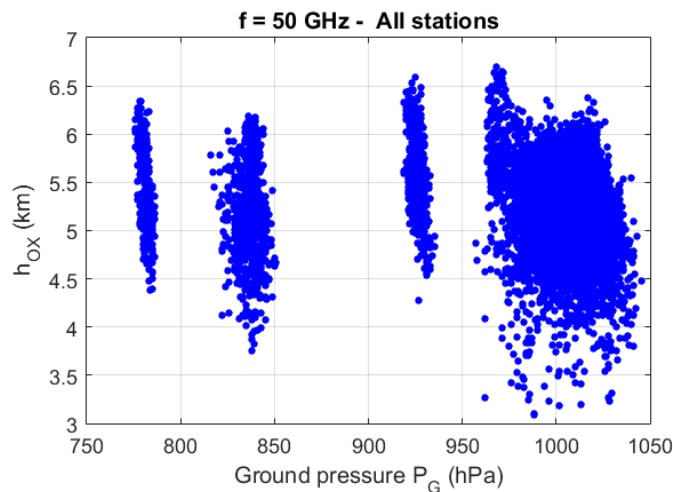

Fig. 6. Correlation between the ground pressure P_G and h_{OX} at $f = 50$ GHz (all stations considered).

4) Total path attenuation

As anticipated in Section II.C2, the zenithal path attenuation due to oxygen A_{OX} (dB) can be calculated with good accuracy from the knowledge of the ground specific attenuation and the oxygen scale height. Hence, we propose the following expression to calculate the attenuation due to oxygen, exceeded with probability, p, between 0.005 and 1 (absolute value), in an average year, along a link with elevation angle θ between 5° and 90°:

$$A_{OX}(p) = \frac{\gamma_{OX}(f,\overline{T}_G, v_G(p), \overline{P}_G) h_0(f, \overline{T}_G, v_G(p))}{\sin\theta} \quad (4)$$

The specific attenuation due to oxygen is calculated according to the MPM93 model/Annex 1 of Recommendation P.676-11, while the oxygen scale height is given by

$$h_0(f, \overline{T}_G, v_G(p)) = 10.27 e^{-\left(\frac{f-61.15}{1.58}\right)^2} + 8.87 e^{-\left(\frac{f-118.75}{1.44}\right)^2}$$
$$+ 6.1 \cdot 10^{-3} f + 0.36 [v_G(p)]^{0.54} - 1.5 \cdot 10^{-4} \overline{T}_G + 3.28 \quad (5),$$

and depends on frequency, as well as on the ground temperature and water vapor content, on the basis of the correlations pointed out in the previous section. As is clear from (4) and (5), aiming at devising a prediction model of simple applicability, we opted for a compromise between accuracy and complexity. Indeed, both y_{OX} and h_{OX} receive as input mean yearly values as for ground temperature and pressure, while only the ground water vapor content is provided in statistical terms (CCDF). A further simplification to the model comes from the fact that, given the reduced impact of pressure on both y_{OX} and h_{OX}, $\overline{P}_G$ (hPa) can actually be calculated assuming a standard atmospheric pressure at the mean sea level of 1013.25 hPa [17] and the following exponential profile for pressure (confirmed by the full RAOBS dataset) [18]:

$$\overline{P}_G = \overline{P}_0 e^{-\frac{h_S}{\overline{h}_P}} = 1013.25 e^{-\frac{h_S}{7.6}} \quad (6)$$

where h_S is the site altitude in km. The RAOBS analysis pointed out that the variation of h_P is quite limited, both throughout the year, and from site to site. Indeed the standard deviation of h_P (all sites, all profiles) is 0.23 km, which increases the significance of the average value $\overline{h}_P = 7.6$ km.

The coefficients in (5) were derived using an optimization procedure aiming at maximizing the agreement between the CCDF of A_{OX}, as calculated from the RAOBS dataset and the MPM93 model (frequencies in the range 10-350 GHz) and as estimated using (4) ($\overline{T}_G$ and $v_G(p)$ are extracted from RAOBS data, while $\overline{P}_G$ is calculated according to (6)). It is worth pointing out that only half of the 24 sites (see the 12 circles in Fig. 7) were actually selected to regress the coefficients in (5), while the remaining locations (12 asterisks) were employed only to perform independent tests on the model's prediction accuracy, as thorough reported in the next section.
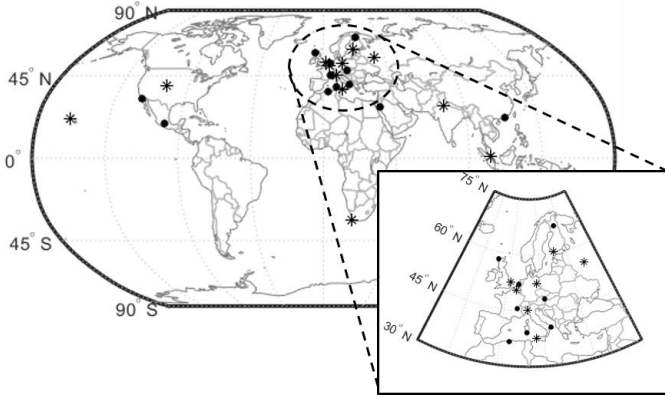
Fig. 7. Sites where RAOBS data were collected: locations denoted with circles used to tune and test the model in (4), remaining ones only to perform tests.

As a final remark, equation (4) indicates that the slant path attenuation is scaled from the zenith to the link elevation angle θ ($5° \leq \theta \leq 90°$) using the simple cosecant law, as also recommended in the Annex 2 of ITU-R P.676-11 [11]. For elevation angles below 5°, the Annex 1 model, fed with full vertical profiles and taking into account also ray-bending effects, should be used [11].

IV. PREDICTION ACCURACY ASSESSMENT

The accuracy of the new model proposed in (4) in predicting the path oxygen attenuation is evaluated here against the RAOBS dataset described in Section II. Fig. 8 reports an example of the vertical (90° elevation angle) oxygen attenuation statistics at 70 GHz, as calculated using the MPM93 model (inputs are the full ROABS profiles), and as derived using the expression in (4) (data relative to Sodankyla, Finland). Another prediction example is given in Fig. 9, but for a site with dry climate (Tabuk, Saudi Arabia) and $f = 70$ GHz. For the sake of comparison, both figures also include the mean yearly value of A_{OX} as predicted using Annex 2 of ITU-R P.676-11.

The performance of the proposed model is quantified in terms of average (E) and root mean square (RMS) values (also reported in the legend of Fig. 8 and Fig. 9) of the ε in (7) (derived by ITU-R in recommendation P.311-15 to compare tropospheric attenuation statistics [19], but multiplied by 100):

$$\varepsilon(p) = \begin{cases} 100\left(\dfrac{A_{ox}(p)}{10}\right)^{0.2} \ln\left(\dfrac{A_{ox}^*(p)}{A_{ox}(p)}\right) & A_{ox}(p) < 10 \text{ dB} \\ 100\ln\left(\dfrac{A_{ox}^*(p)}{A_{ox}(p)}\right) & A_{ox}(p) \geq 10 \text{ dB} \end{cases} \quad (\%) \quad (7)$$

where $A_{OX}^*(p)$ and $A_{OX}(p)$ are the oxygen attenuation values extracted from the estimated and reference attenuation statistics, respectively, for the same probability level $p \geq 0.005$.

Fig. 10 summarizes the performance of the proposed prediction model by showing the average E (ψ_E) and average RMS (ψ_{RMS}) values as a function of frequency. Results

highlight a good accuracy (overall $\psi_{RMS} = 5.8$), which shows a slight bias ($\psi_E = -2.1$) and a peak ψ_{RMS} of approximately 11 for $f = 90$ GHz. Fig. 11 complements the assessment of the model's accuracy by showing the performance as a function of the site: rather small site-to-site variation emerges, with ψ_{RMS} ranging from roughly 5.3 to 8.4.
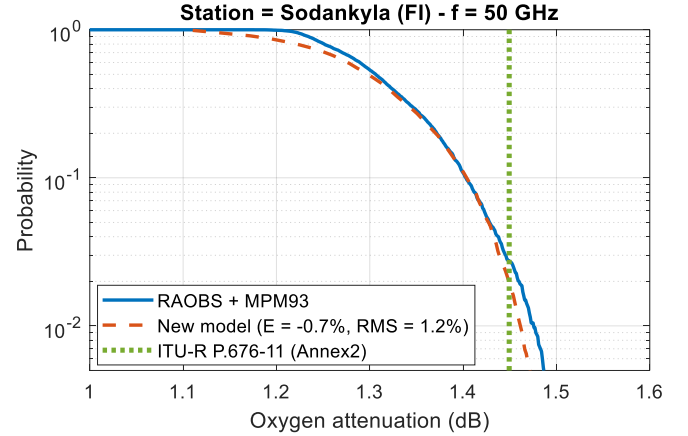

Fig. 8. Zenithal oxygen attenuation CCDF at 50 GHz calculated according to the MPM93 model using as input full RAOBS vertical profiles (blue solid line) and according to the new approximate expression in (4) (dashed red line). Also reported is the mean yearly value of A_{OX} as predicted using Annex 2 of ITU-R P.676-11 (green dotted line). Site: Sodankyla, Finland.
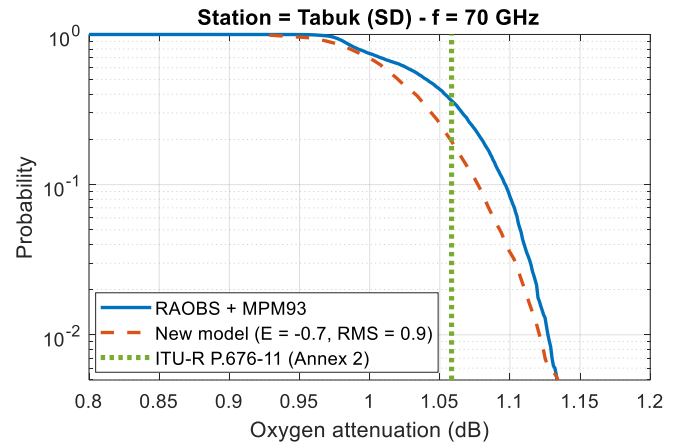

Fig. 9. Zenithal oxygen attenuation CCDF at 70 GHz calculated according to the MPM93 model using as input full RAOBS vertical profiles (blue solid line) and according to the new approximate expression in (4) (dashed red line). Also reported is the mean yearly value of A_{OX} as predicted using Annex 2 of ITU-R P.676-11 (green dotted line). Site: Tabuk, Saudi Arabia.

For the results shown in Fig. 10 and Fig. 11, both $\overline{T}_G$ and $v_G(p)$ were extracted from RAOBS data as well (level closer to the ground). In the light of applying the model on worldwide basis taking advantage of global meteorological databases already available, the model was also tested using the following input values:

- for the ground water vapor content: the CCDF of $v_G(p)$, extracted from the ERA40 database of the European Centre for Medium-Range Weather Forecast (ECMWF), currently included in recommendation ITU-R P.836-5

This article has been accepted for publication in a future issue of this journal, but has not been fully edited. Content may change prior to final publication. Citation information: DOI 10.1109/TAP.2017.2765541, IEEE Transactions on Antennas and Propagation

> REPLACE THIS LINE WITH YOUR PAPER IDENTIFICATION NUMBER (DOUBLE-CLICK HERE TO EDIT) <   7

[12] (spatial resolution: 1.125°×1.125°);

- for the ground temperature: mean yearly values extracted again from the ERA40 database, but not yet included in any ITU-R recommendation (however, the digital map of $\overline{T}_G$, but with spatial resolution of 1.5°×1.5°, is currently attached to recommendation ITU-R P.1510-0 [13]).
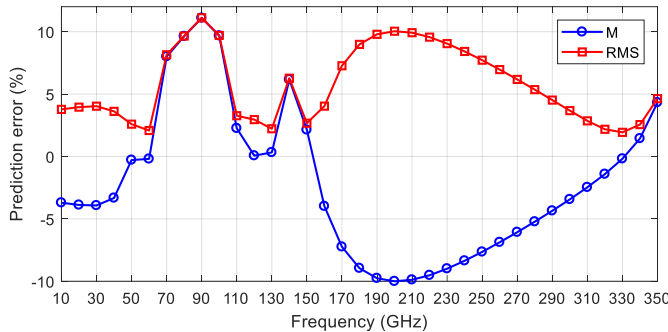

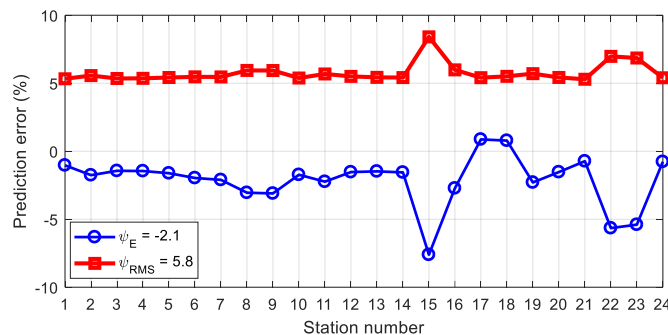Fig. 10. Mean E (ψ_E) and mean RMS (ψ_{RMS}) as a function of frequency (average over all stations).

Fig. 11. Mean E (ψ_E) and mean RMS (ψ_{RMS}) as a function of the RAOBS site (average over all frequencies).

The results obtained using such NWP products are very similar to those reported in Fig. 10 and Fig. 11: the trends of ψ_E and ψ_{RMS}, both with frequency and with site, are the same, but the overall score shows just a slight worsening ($\psi_E = -2.9$ and $\psi_{RMS} = 6.1$). This corroborates the use of the proposed model for the prediction of A_{OX} statistics, which represents a significant improvement over the approximate prediction method currently proposed in Annex 2 of recommendation ITU-R P.676-11.

V. CONCLUSIONS

This contribution presents a simplified yet accurate model for the prediction oxygen attenuation at millimeter-wave on Earth-space links, which receives as input simple local meteorological information, namely the mean yearly ground temperature $\overline{T}_G$ and the statistics of ground water vapor content $v_G(p)$. Taking advantage of an extensive set of RAOBS ascents collected in several sites worldwide and characterized by high accuracy and reliability, the model is devised by investigating and modeling the dependence of the oxygen equivalent scale height on frequency, as well as on $\overline{T}_G$ and

$v_G(p)$, while the ground specific oxygen attenuation is calculated according to the accurate formulation included in the Liebe's MPM93 mass absorption model.

The proposed model, tested against reference oxygen attenuation statistics obtained using the Liebe MPM93 model coupled with the mentioned RAOBS dataset, shows a very satisfactory accuracy, both in terms of overall prediction error (average ψ_{RMS} equal to 5.8, considering all sites and all frequencies), as well as in terms of performance stability, which turns out to be slightly dependent on frequency, and almost independent of the considered site.

REFERENCES

[1] A. Botta, A. Pescape, "On the performance of new generation satellite broadband internet services," *IEEE Communications Magazine*, pp. 202-209, Vol. 52, Issue 6, 2014.

[2] J.E. Allnutt, "*Satellite to ground radiowave propagation*," 2nd edition, the IET.

[3] C. Riva, C. Capsoni, L. Luini, M. Luccini, R. Nebuloni, A. Martellucci, "The Challenge of Using the W Band in Satellite Communication," *Int. J. Satell. Commun. Network.*, 2014; 32:187–200.

[4] L. Luini, C. Capsoni, R. Nebuloni, "Free Space Optics to Enable High Data Rate Download from LEO Satellites: the Impact of Clouds", *3rd International Workshop on Optical Wireless Communications – 2014 (IWOW2014)*, pp. 35-39, 17-19 September 2014, Funchal, Madeira, Portugal.

[5] P. Bouchard, "Approximate method for estimating gaseous loss at very low angles along paths of finite length and earth-space paths," *IEEE Trans. Antennas Propag.*, vol. 64, no. 2, pp. 687–699, Feb. 2016.

[6] H. J. Liebe, G. A. Hufford, M. G. Cotton, "Propagation modeling of moist air and suspended water/ice particles at frequencies below 1000 GHz," *in Proc. AGARD 52nd Spec. Meeting EM Wave Propag.*.

[7] P. Rosenkranz, "Water vapor microwave continuum absorption: A comparison of measurements and models," *Radio Sci.*, vol. 33, no. 4, pp. 919–928, Jul./Aug 1998.

[8] A. Berk et al., "MODTRAN4 radiative transfer modeling for atmospheric correction," Proc. SPIE, vol. 3756, pp. 348-353, Oct. 1999.

[9] LBLRTM. accessed on Nov. 2016. [Online]. Available: http://rtweb.aer.com/lblrtm.html.

[10] J. Sun, F. Hu, S. Lucyszyn, "Predicting atmospheric attenuation under pristine conditions between 0.1 and 100 THz," IEEE Access, vol. 4, pp. 9377-9399, Nov. 2016.

[11] ITU-R recommendation P.676-11, "Attenuation by atmospheric gases," Geneva, Switzerland, 2016.

[12] ITU-R recommendation P.836-5, "Water vapour: surface density and total columnar content," Geneva, Switzerland, 2013.

[13] ITU-R recommendation P.1510-0, "Annual mean surface temperature," Geneva, Switzerland, 2001.

[14] COST Action 255 Final Report, "Precipitation, Clouds and Other Related Non-Refractive Effects," J. P. V. Poiares Baptista, Ed. Noordwijk, The Netherlands: ESA Publication Division, ch. 3.2.

[15] ITU-R recommendation P.840-6, "Attenuation due to clouds and fog," Geneva, Switzerland, 2013.

[16] ITU-R, "Radio Regulations," Geneva, Switzerland, November 2016.

[17] *International Organization for Standardization*, Standard Atmosphere, ISO 2533:1975, 1975.

[18] L. Luini, C. Capsoni, "Using NWP Reanalysis Data for Radiometric Calibration in Electromagnetic Wave Propagation Experiments," *IEEE*

Transactions on Antennas and Propagation, vol. 64, no. 2, Page(s): 700 - 707, February 2016.

[19] ITU-R recommendation P.311-15, "Acquisition, presentation and analysis of data in studies of tropospheric propagation," Geneva, Switzerland, 2015.